

¹Songhan Pang¹Jian Liu²Kuikui Wu³Hongqi Zhang

Three-Level Midpoint Potential Balance and Harmonic Suppression Strategy Under Low Carrier Ratio



Abstract: - An improved virtual space vector modulation method is proposed to address the issues of output voltage distortion and high harmonic content caused by unbalanced midpoint potential in the application of diode midpoint clamped three-level inverters in high-speed motor drive scenarios. Firstly, based on the potential difference of the voltage divider capacitor, the average value of the midpoint current that needs to flow out is determined to allocate the action time of the positive and negative virtual small vectors, so as to make the potential difference of the voltage divider capacitor approach zero and achieve midpoint potential balance control. Secondly, the virtual vector losing its midpoint potential balance suppression effect due to angle and sampling delay in high-speed permanent magnet synchronous motors, and considering that traditional methods do not use virtual small vectors in the high modulation ratio range ($0.667 < m < 1$), this paper re divides the reference voltage vector interval to avoid the voltage reference vector falling into the high modulation ratio range and causing the midpoint potential to lose balance. Finally, a simulation model was constructed to validate the proposed strategy, and the simulation results showed that the proposed method can effectively reduce the harmonic content of line voltage and current by suppressing the midpoint potential balance.

Keywords: High speed permanent magnet synchronous motor; three-level; midpoint clamp inverter; virtual space vector pulse width modulation; voltage balance

0 Preface High-speed motors are widely used in fields such as aerospace and manufacturing due to their advantages of high power density and high working efficiency [1-2]. The characteristic of high operating fundamental frequency of high-speed motors leads to a lower carrier ratio in the control system of high-speed motors compared to ordinary motor control systems. The angle and sampling delay become more pronounced in the control system with a low carrier ratio, thereby resulting in an increase in harmonic content. Three-level inverters increase the number of levels by adding power devices, making the output voltage waveform closer to a sine wave and can effectively reduce harmonic content. They have been widely used in medium and high voltage drive scenarios [3-4]. The change of the neutral current when the Neutral Point Clamped (NPC) three-level inverter outputs voltage causes an unbalanced voltage of the upper and lower divider capacitors at the neutral point, resulting in distorted output voltage and large harmonic content of the inverter.

The neutral point balance issue is an unavoidable problem when using NPC three-level inverters and is also a hot research topic for scholars at home and abroad [5-7]. The zero-sequence voltage injection method achieves neutral point potential balance by injecting zero-sequence voltage into the three-phase modulation waves and is one of the common methods for neutral point potential balance [8-9]. However, this method requires complex calculations using parameters such as three-phase reference voltage, output current, and DC bus voltage, and is not suitable for application in high-frequency scenarios such as high-speed motor control systems. Achieving neutral point potential balance based on space vector pulse width

¹ School of Electrical and Electronic Engineering, Shandong University of Technology, Zibo Shandong 25500, China;

² Zhejiang Jiafeng Power Technology Co., Ltd., Jiaxing Zhejiang 314019, China;

³ Shandong Shanbo Electric Machine Group Co., Ltd., Zibo Shandong 255299, China)

^aEmail: sddepsh@163.com

^bEmail: 1780883082@qq.com

^cEmail: wkk@jfpowerchina.com

^dEmail: zgq_Zhang8169SDUT@163.com

*Corresponding author

modulation (SVPWM) is also one of the common means [10]. In the three-level vector space, medium and small vectors cause changes in the neutral current and have the most obvious influence on the neutral point potential. Literature [11] utilizes the feature that positive and negative small vectors generate opposite neutral currents for neutral point potential balance, but this method does not consider the influence of medium vectors on the neutral point potential. Medium vectors do not exist in pairs like small vectors. Literature [12] chooses not to use medium vectors for modulation, but without the participation of medium vectors in modulation, there is no conversion of adjacent vectors, which leads to exacerbated voltage distortion and an increase in harmonic content. Literature [13] utilizes medium vectors and small vectors to form a virtual vector with an average current flowing out of the neutral point being zero, known as virtual space vector pulse width modulation (virtual space vector pulse width modulation, VSVPWM) or the Nearest Three Virtual Vectors (NTV2). It has been theoretically proven that all virtual vectors have no influence on the neutral point. However, VSVPWM only suppresses the change of the neutral point voltage and does not have the function of controlling the neutral point potential balance. Moreover, in practical applications, the small inductance of high-speed motors leads to an increase in the current ripple of the control system, affecting the symmetry of the three-phase current, and the virtual medium vector loses its ability to suppress the neutral point potential balance. Literature [14] proposed a method to select different small vectors based on the neutral point voltage on the basis of the virtual space vector. Similarly, methods of introducing a balance factor into the virtual small vector have also been proposed by some scholars [15-17]. These methods all perform neutral point potential balance control by utilizing the characteristic that paired small vectors have opposite influences on the neutral point potential. However, within the vector interval with a large modulation ratio ($0.667 < m < 1$), there are no paired small vectors, so the neutral point potential balance effect of this control method within these vector intervals is not ideal. To solve this problem, literature [18] proposed a variable virtual medium vector method and introduced a balance factor to define the virtual medium vector. Thus, within the modulation interval where the virtual small vector is ineffective, the variable virtual medium vector can be used for modulation to control the neutral point potential, but the vector interval calculation of this method becomes more complex due to the existence of the variable virtual medium vector, increasing the calculation amount within the unit sampling time.

This paper presents an improved virtual space vector modulation technique based on high speed permanent magnet synchronous motor. This paper firstly analyzes the influence of the control system of high speed permanent magnet synchronous motor on the traditional VSVPWM. At the same time, in order to solve the problem that the virtual medium vector can not play the role of suppressing the midpoint potential drift in the medium and high modulation ratio interval ($0.667 < m < 1$), a new method was proposed to divide the vector interval and change the modulation rule of the virtual vector. This method overcomes the deficiency that VSVPWM can not balance the midpoint potential in the middle and high modulation ratio range, and can effectively reduce the harmonic content of the system, which is more suitable for low carrier ratio driving applications than the traditional scheme. Finally, the phase-duty ratio method is used to reduce the switching frequency effectively, which solves the problem that VSVPWM each phase of the bridge arm switch state switching times. Simulation results show that the proposed method is feasible and effective.

1 NPC Three level inverter

Figure 1 shows the topology of a three-level inverter, with each bridge arm consisting of four power switching tubes and two clamping diodes. Each bridge arm can output three levels, taking phase a as an example, when switching tubes S1 and S2 are turned on, S3 and S4 are turned off, the output level of phase a is, denoted as output state P; when switching tubes S2 and S3 are turned on, S1 and S4 are turned off, the output level of phase a is, denoted as output state O; when switching tubes S1 and S2 are turned off, S3 and S4 are turned on, the output level of phase a is, Denoted as output state N.

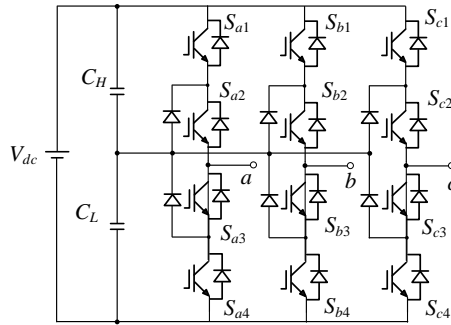


Fig.1 NPC Three-level inverter

Since each phase of a three-level circuit can output P,O, and N three states, a total of three phases can output a switching state. The space voltage vector corresponding to each switching state is

$$V = \frac{2}{3}(v_a + v_b e^{j\frac{2\pi}{3}} + v_c e^{j\frac{4\pi}{3}}) \tag{1}$$

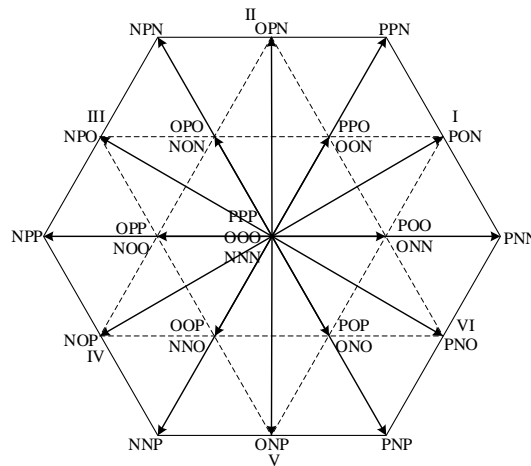


Fig.2 space vector diagram for NPC converter

The vector space diagram composed of 27 vectors is shown in Figure 2. According to the vector's modulus length, 27 basic space vectors can be divided into four categories: long vector, medium vector, small vector and zero vector. Except for the zero vector and the long vector, the other vectors all have an influence on the midpoint voltage. Table 1 shows the midpoint current of different small vectors, medium vectors and their action. The midpoint current caused by different basic space vectors is different, which is also the direct reason for affecting the balance of the midpoint potential.

Tab.1 Neutral point current for medium and small vectors

Positive small vector	i_{np}	Negative small vector	i_{np}	Middle vector	i_{np}
POO	$-i_a$	ONN	i_a	PON	i_b
PPO	i_c	OON	$-i_c$	OPN	i_a
OPO	$-i_b$	NON	i_b	NPO	i_c
OPP	i_a	NOO	$-i_a$	NOP	i_b
OOP	$-i_c$	NNO	i_c	ONP	i_a
POP	i_b	ONO	$-i_b$	PNO	i_c

2 Effect of low carrier ratio on VSVPWM

The traditional virtual space vector balancing algorithm synthesises a new virtual vector by combining the basic vectors, so that the average current of the new virtual vector is zero. This method can effectively suppress the midpoint potential drift in theory, and can also ignore the influence of non-ideal factors such as delay in the ordinary motor control system, so as to obtain a good suppression effect of midpoint potential drift. However, in the control system of high speed permanent magnet synchronous motor, the delay of sampling and Angle cannot be ignored due to the influence of low carrier ratio.

The fundamental frequency of high speed permanent magnet synchronous motor is high, but due to the limitation of the power switch tube itself, the sampling frequency cannot increase indefinitely with the increase of fundamental frequency. Therefore, the permanent magnet synchronous motor control system carrier ratio is low. Under such conditions, the sampled phase current may be significantly different from the actual phase current when the neutral point potential balancing action is applied with the phase current.

After a delay of 1.5 times the sampling time, the electrical position movement of the rotor can be expressed as

$$\theta_{adv} = 1.5\omega_0 T_s \quad (2)$$

Where, T_s represents a sampling period; ω_0 indicates the fundamental frequency. For the convenience of demonstration, the sampling frequency is assumed to be 16kHz and the fundamental wave frequency is 1kHz.

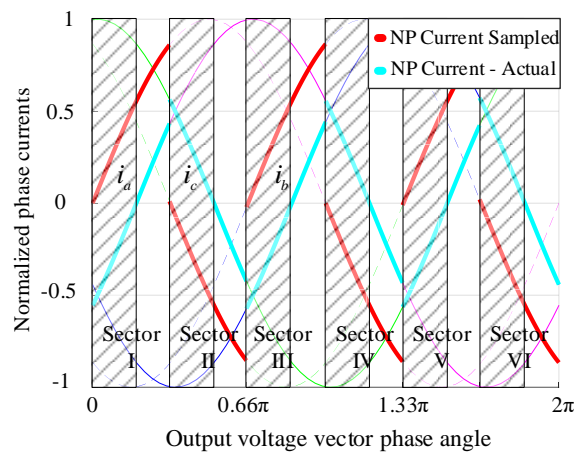


Fig.3 Variation of NP current

When the carrier ratio is low, the current value cannot be considered unchanged after a delay of 1.5 sampling cycles. Figure 3 shows the three-phase current after 1.5 sampling period delay, and the bold part is the current used by the virtual small vector in this sector to balance the midpoint potential. As can be seen from the figure, the problem of sampling delay will cause the polarity of the actual current value and the sampled current value to be opposite, as shown in the shaded part in Figure 3. In this case, the suppression effect of the midpoint potential drift of the virtual small vector will be weakened.

At the same time, the calculation period of the current loop and the velocity loop also requires a certain calculation time, which will lead to a certain deviation between the output voltage after space vector modulation and the actual voltage required, which will lead to an error between the current of the motor winding and the ideal current value, and to a certain extent, the sampled current value is inconsistent with the actual value of the three-phase current. In most cases, sampling the two current sensors to obtain the third phase current value will cause a certain degree of three-phase current imbalance, so the average value of the midpoint current caused by using the virtual vector in a single sampling period is not zero. Therefore, the virtual medium vector can not only inhibit the midpoint potential drift, but aggravate the imbalance of midpoint potential, so the use of virtual medium vector should be reduced as much as possible.

3 Improved VSPWM method

3.1 Virtual space vector definition

Taking the I large sector as an example, the balance factor is added to overcome the shortcoming of traditional VSPWM without midpoint voltage balance control strategy, and the virtual small vector is defined as

$$\begin{cases} V_{VS1} = k_{VS1}V_{ONN} + (1-k_{VS1})V_{POO} \\ V_{VS2} = k_{VS2}V_{OON} + (1-k_{VS2})V_{PPO} \end{cases} \quad (3)$$

Where k_{VS1} and k_{VS2} are constants, and represents the fundamental vector.

The midpoint current is analyzed:

$$\begin{cases} i_{np_VS1} = k_{VS1}i_{ONN} + (1-k_{VS1})i_{POO} = i_a(2k_{VS1} - 1) \\ i_{np_VS2} = k_{VS2}i_{OON} + (1-k_{VS2})i_{PPO} = i_c(1 - 2k_{VS2}) \end{cases} \quad (4)$$

Obviously, when both k_{VS1} and k_{VS2} are 1/2, the average current flowing out of the midpoint during the sampling time can be guaranteed to be zero.

Using the basic medium vector and the small vector of the sector, the virtual medium vector is defined as

$$V_{VM} = \frac{1}{3}V_{PNN} + \frac{1}{3}V_{PON} + \frac{1}{3}V_{PPO} \quad (5)$$

The midpoint current is analyzed:

$$i_{np_VM} = \frac{1}{3}i_{ONN} + \frac{1}{3}i_{PON} + \frac{1}{3}i_{PPO} = \frac{1}{3}(i_a + i_b + i_c) \quad (6)$$

$$\text{In one sampling period, ideally, there is } i_a + i_b + i_c = 0 \quad (7)$$

Therefore, under ideal circumstances, the mean value of the outgoing midpoint current during the sampling time can be guaranteed to be zero when the virtual medium vector is used for modulation.

The basic vectors of the long vector and the zero vector are directly treated as virtual vectors, i.e

$$\begin{cases} V_{VL1} = V_{PNN} \\ V_{VL2} = V_{PPN} \\ V_{V0} = V_{OOO} \end{cases} \quad (8)$$

3.2 The virtual small vector of midpoint voltage control method

In theory, the virtual vector defined in the previous section can ensure that the current flowing out of the midpoint per unit sampling time is zero, but in practice, it is affected by many factors such as Angle delay and sampling delay, resulting in the imbalance of the midpoint voltage. The main reason is that the traditional method only tries to suppress the balance of the midpoint potential rather than actively control it.

It is not difficult to find from equation (4) that when virtual small vectors are used for modulation, the value of the coefficient can be changed to control the size of the outgoing midpoint current. During the operation time of the virtual small vector, the current flowing out of the midpoint can be expressed as

$$\begin{aligned} \int_{T_m}^{T_{m+1}} i_{np} dt &= i_{VS_P}T_{VS_P} + i_{VS_N}T_{VS_N} = T_{VS}k_{VS}i_{VS_N} \\ &+ (1 - k_{VS})T_{VS}i_{VS_P} = (2k_{VS} - 1)i_{VS_N}T_{VS} \end{aligned} \quad (9)$$

Where is the current flowing out of the midpoint, and represents the current flowing out of the midpoint when the basic positive small vector and negative small vector respectively, and represents the time of the basic positive small vector and negative small vector respectively.

The midpoint voltage change is expressed as

$$\square(U_{C1} - U_{C2}) = \frac{1}{C} q_{out} = \frac{1}{C} \int_{T_{sn}}^{T_{sn+1}} i_{np} dt \quad (10)$$

It can be obtained by formula (9)-(10).

$$\square(U_{C1} - U_{C2}) = \frac{1}{C} (2k_{VS} - 1) i_{VS-N} T_{VS} \quad (11)$$

And respectively represent the voltage of the partial voltage capacitor and the capacitance value of the partial voltage capacitor. Assuming that the current capacitor voltage difference between the upper and lower midpoint is, the midpoint voltage can be compensated by changing the deviation caused by the midpoint voltage, which can be expressed by equation (11) as.

$$k_{VS} = \frac{-\square UC + i_{VS-N} T_{VS}}{2i_{VS-N} T_{VS}} \quad (12)$$

With formula (12), the value calculated at each sampling period can be realized to control the midpoint voltage.

3.3 Reference voltage vector region division

According to the definition of traditional virtual space vector, the large sector can be divided into 5 regions as shown in Figure 4 (a), and the three nearest virtual vectors in the region where the reference vector resides are selected for modulation. According to the above rules, it is not difficult to find that when the reference voltage vector is located in other small sectors except small sector 1, the virtual medium vector will participate in modulation, and the virtual small vector is not used for modulation in small sector 4, and the balance factor cannot play a controlling role. The traditional region division method is not conducive to the control of the balance of the midpoint potential.

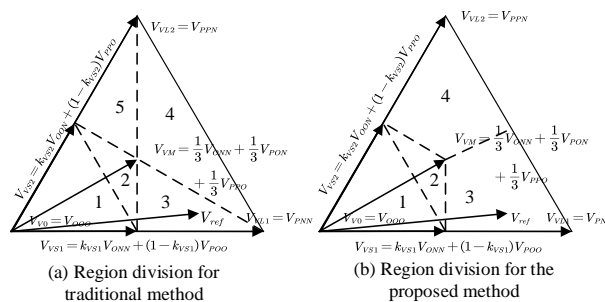


Fig.4 Region division

As described in Section 2, the use of virtual medium vectors in high-speed motor modulation methods should be avoided to reduce the influence on the midpoint voltage and virtual small vectors should be used as much as possible to exert balance factor control. Therefore, it is necessary to redivide the small sectors.

As shown in Figure 4(b), small sectors 1 and 2 are still the same as the traditional algorithm. If the reference vector is in the small sectors 3 and 4, the virtual small vector and long vector adjacent to the small sector and another virtual long vector are selected as the vectors participating in the synthesis. In this way, medium vectors are not required in all small sectors except small sector 2, and each sector can be modulated with small vectors to control the midpoint voltage.

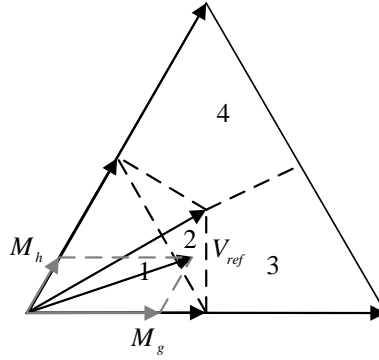


Fig.5 Region division for the proposed method

The proposed method determines the region of the reference vector as follows. The target reference vector is decomposed as shown in Figure 5, and the decomposed vector can be expressed as

$$\begin{cases} M_g = \frac{\sqrt{3}}{2U_{DC}}(V_{ref} \cos \theta_{ref} - V_{ref} \sin \theta_{ref}) \\ M_h = \frac{\sqrt{3}}{U_{DC}}V_{ref} \sin \theta_{ref} \end{cases} \quad (13)$$

According to Figure 5 and equation (13), the small sector in which the reference voltage vector resides can be determined according to the conditions satisfied by the modulation ratio and rotation Angle of the target vector. The specific judgment basis is given in Table 2.

Tab.2 Reference voltage region identification strategy

Region	Condition for M_g and M_h
1	$M_g + M_h \leq 0.5$
2	$M_g + M_h > 0.5$ 且 $M_g < 0.5$ 且 $M_h < 0.5$
3	$M_g > 0.5$ 且 $M_h > 0.5$ 且 $M_g \geq M_h$
4	$M_g > 0.5$ 且 $M_h > 0.5$ 且 $M_g < M_h$

3.4 Reference voltage vector synthesis

According to the region division rules in the previous section, determine the three virtual vectors used to synthesize the reference voltage vector. When the reference vector falls in small sector 1 and 2, the vector selection method is the same as the traditional vector synthesis time. When the reference vector falls in small sector 3 and small sector 4, the virtual small vector and long vector present in the current sector are selected and another virtual long vector is used for vector synthesis. Take small sector 3 as an example, according to the above method, select, and, according to the volt-second balance principle

$$\begin{cases} V_{ref} = V_{VS1}T_{VS1} + V_{VL1}T_{VL1} + V_{VL2}T_{VL2} \\ T_{VS1} + T_{VL1} + T_{VL2} = T_s \end{cases} \quad (13)$$

T_{VS1} 、 T_{VL1} and T_{VL2} respectively V_{VS1} 、 V_{VL1} and V_{VL2} According to equation (13), the time for each vector to participate in vector synthesis is.

$$\begin{cases} T_{VS1} = 2 - 2M \sin(\theta + \pi/3) \\ T_{VL1} = \sqrt{3}M \cos \theta - 1 \\ T_{VL2} = M \sin \theta \end{cases} \quad (14)$$

3.5 Analysis and optimization of switching frequency

The proposed method still uses the traditional virtual space vector to synthesize the target vector in small sectors 1 and 2, and can still follow the traditional method in determining the switching order. In small sectors 3 and 4, taking small sector 3 as an example, the virtual vector of the synthesized target vector is V_{VS1} 、 V_{VL1} and V_{VL2} , The basic vector that we need to use is V_{ONN} 、 V_{POO} 、 V_{PNN} 、 V_{PPN} 。 In order to ensure the minimum switching times and symmetry in sampling time, the order of vector action in small sector 3 is defined as V_{PPN} 、 V_{PNN} 、 V_{ONN} 、 V_{POO} 、 V_{ONN} 、 V_{PNN} 、 V_{PPN} 。 Similarly, the order of vector action for small sector 4 can be obtained. Taking sector I as an example, the switching sequence of each small sector is shown in Table 3. The switching sequence of other large sectors is similar to that of sector I.

Tab.3 Pulse pattern for sector I

Region	Pulse sequence
1	$V_{PPO} \rightarrow V_{POO} \rightarrow V_{OOO} \rightarrow V_{OON} \rightarrow$ $V_{ONN} \rightarrow V_{OON} \rightarrow V_{OOO} \rightarrow V_{POO} \rightarrow V_{PPO}$
2	$V_{PPO} \rightarrow V_{POO} \rightarrow V_{PON} \rightarrow V_{OON} \rightarrow$ $V_{ONN} \rightarrow V_{OON} \rightarrow V_{PON} \rightarrow V_{POO} \rightarrow V_{PPO}$
3	$V_{PPN} \rightarrow V_{PNN} \rightarrow V_{ONN} \rightarrow V_{POO} \rightarrow$ $V_{ONN} \rightarrow V_{PNN} \rightarrow V_{PPN}$
4	$V_{PNN} \rightarrow V_{PPN} \rightarrow V_{PPO} \rightarrow V_{OON} \rightarrow$ $V_{PPO} \rightarrow V_{PPN} \rightarrow V_{PNN}$

4 Simulation verification

In order to verify the effectiveness of the midpoint balance control method proposed in this paper, a three-level drive control system of a high-speed permanent magnet motor with a speed of 32krpm was built in simulink. Detailed parameters of the prototype are shown in Table 4.

Tab.4 System parameters

System parameters	Value
$n/(r/min)$	32000
L_s/mH	0.675
ψ_f/Wb	0.0406
R/Ω	0.122
P_n	1
$J/kg \cdot m^2$	1.75×10^{-5}

In the actual application process, the upper and lower capacitors can not be exactly the same, so the partial voltage capacitor itself has a certain potential deviation. Therefore, the initial value of the voltage of the upper and lower capacitors is $U_{dc} / 2 + 10$ and $U_{dc} / 2 - 10$, The voltage difference between the upper and lower capacitors is 20V to simulate this phenomenon. FIG. 8 and FIG. 12 are simulation experiments under traditional VSVPWM modulation. FIG. 9 and FIG. 13 are simulation experiments using only virtual small vector control midpoint voltage balance method (hereinafter referred to as small vector balance method). FIG. 10 and FIG. 14 show the simulation experiments under the modulation of the proposed method

As mentioned above, the traditional VSVPWM method only avoids the occurrence of unbalance as far as possible under the condition that the midpoint potential has been balanced, and does not actively control the unbalance phenomenon. This is confirmed by the capacitive voltage balancing process shown in Figure 6(a). The unbalance of the midpoint potential will undoubtedly distort the output voltage, so the traditional VSVPWM method has great limitations in use. In order to facilitate the subsequent comparison of the midpoint potential balance effect, simulation waveforms without setting the initial capacitor voltage are presented respectively, as shown in FIG. 6(b) and (c).

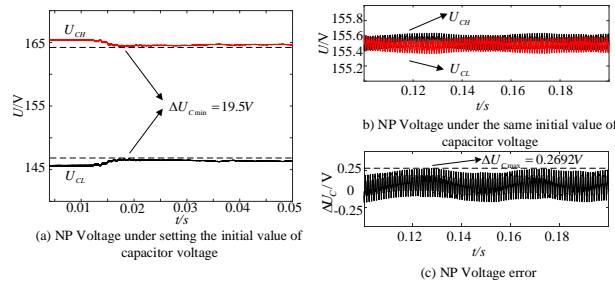


Fig.6 Simulation of midpoint voltage under VSVPWM

When using small vector balance method, the midpoint potential balance effect is significantly improved compared with VSVPWM. Not only is the midpoint potential actively controlled, as shown in FIG. 7(a), but the effect after midpoint potential balance is also significantly improved, as shown in FIG. 7(b) and (c). As can be seen from the figure, the maximum fluctuation voltage after the potential balance at the midpoint is reduced from 0.2692V to 0.1674V. However, as shown in FIG. 7(a), the midpoint potential could not be balanced from 0.25s to 0.4s. FIG. 9(d) shows that during this period, due to relatively large modulation ($0.667 < m < 1$), the reference vector was in the small sector 4 as shown in FIG.4 (a) for most of the time. In this case, the small vector balance method will choose to use the virtual medium vector for modulation, but as mentioned in Section 2, the virtual medium vector not only loses the suppression effect of the midpoint potential drift, but has an impact on the midpoint potential, so the small vector balance method cannot balance the midpoint potential for this situation, which verifies the above theory and indicates the necessity of re-dividing small sectors.

As shown in FIG. 8(a), the proposed method makes up for the shortcomings of the small vector balance method. After the small sectors are redivided, the midpoint potential imbalance as shown in FIG. 7(a) does not occur, which proves that the proposed method can effectively control the midpoint voltage balance in the high modulation interval. As shown in Figure 8(b) and (c), the voltage fluctuation after the midpoint balance is further reduced to 0.1438V.

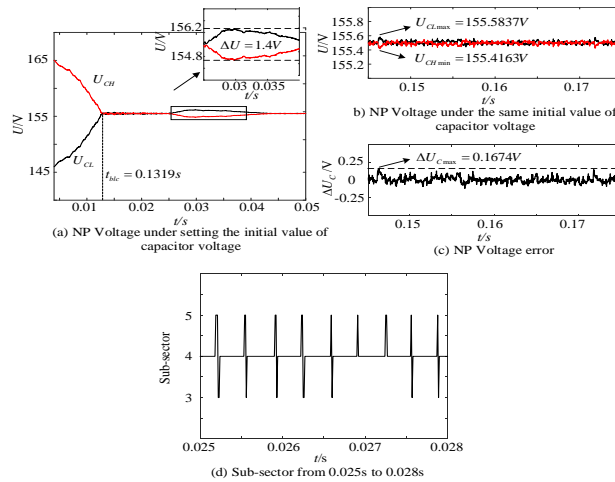


Fig.7 Simulation of midpoint voltage under Small vector balance method

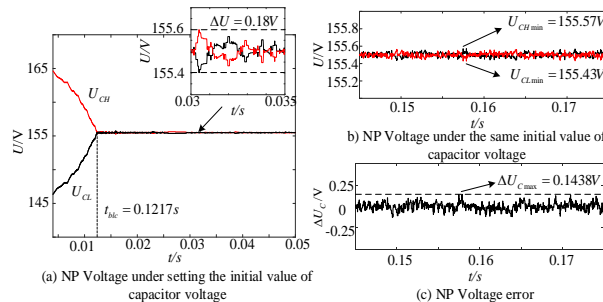


Fig.8 Simulation of midpoint voltage under proposed method

FIG. 9(a) and (b) show the phase current and line voltage simulation experiment harmonic content analysis of VSVPWM algorithm respectively. The THD of the line voltage is 41.98%, the THD of the harmonics below 16 times is 13.47%, and the THD of the output line current is 2.32%.

FIG. 10(a) and (b) show the analysis of harmonic content of phase current and line voltage simulation experiments with small vector balance method respectively. The THD of the line voltage is 39.81%, the THD of only the harmonics below 16 times is 9.5%, and the THD of the output line current is 1.77%. The THD of the output line voltage and phase current is also decreased due to the good control of the midpoint potential.

The harmonic content analysis of the phase current and line voltage simulation experiment of the proposed midpoint potential balance strategy is shown in FIG. 11(a) and (b). The THD of the line voltage is 37.61%, the THD of the harmonics below 16 times is 8.59%, and the THD of the output line current is 1.32%. The simulation results verify that the proposed midpoint potential balancing method can significantly reduce the harmonic content of the system by providing a good control effect of the midpoint potential.

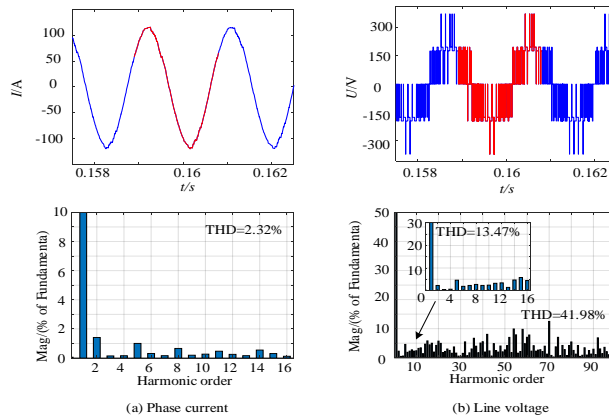


Fig.9 FFT of phase current and line voltage under VSVPWM

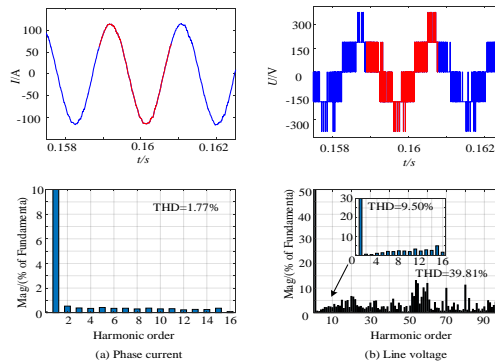


Fig.10 FFT of phase current and line voltage under small vector balance method

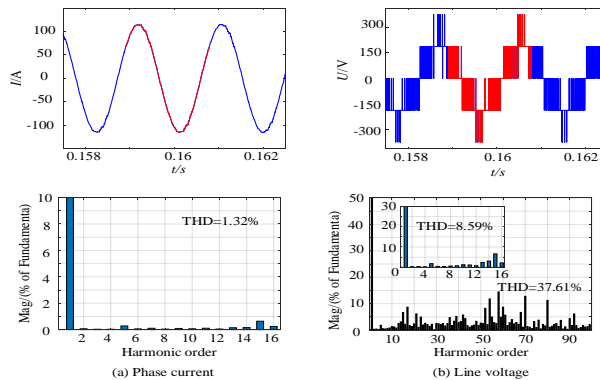


Fig.11 FFT of phase current and line voltage under proposed method

5 CONCLUSION

This paper firstly analyzes the influence of low carrier ratio factor on VSVPWM in the control system of high speed permanent magnet synchronous motor. Then, a strategy of balancing the midpoint voltage with virtual small vector is proposed, and the reference voltage vector region is redivided. The failure of traditional VSVPWM to suppress midpoint potential drift is solved, and the problem that virtual small vector cannot participate in modulation to control midpoint potential balance in the high modulation ratio interval ($0.667 < m < 1$) is solved, and the balance control of midpoint potential in the whole modulation domain is ensured. Finally, the phase-duty ratio method is proposed to solve the problem of high switching times of each phase switch state, which significantly reduces the switching loss. Simulation results show that the proposed method can effectively balance the midpoint potential and reduce the harmonic content of the system. Compared with the traditional VSVPWM method, the output voltage distortion is reduced by about 4.88%, and the output current harmonic is reduced by about 1%.

REFERENCE

- [1] Li Yan. Research on New Weak Field Control of High Speed Permanent Magnet Synchronous Motor for Compressor [J]. *Micro Motor*, 2023, 51(11): 46-51+58.
- [2] J. Ou, Y. Liu and M. Doppelbauer. Comparison Study of a Surface-Mounted PM Rotor and an Interior PM Rotor Made From Amorphous Metal of High-Speed Motors [J]. *IEEE Transactions on Industrial Electronics*, 2021, 68(10): 9148-9159.
- [3] Xu Zhi-Xian, WANG Zheng, WANG Xue-Qing et al. Zero-common-mode Voltage Model Predictive Control for T-type three-level Two-three-phase permanent magnet synchronous Motor [J]. *Proceedings of the CSEE*, 2020, 40(13): 4301-4310.
- [4] V. Viswanathan and J. Seenithangom. Commutation Torque Ripple Reduction in the BLDC Motor Using Modified SEPIC and Three-Level NPC Inverter [J]. *IEEE Transactions on Power Electronics*, 2018, 33(1): 535-546.
- [5] C. Hu et al. An Improved Virtual Space Vector Modulation Scheme for Three-Level Active Neutral-Point-Clamped Inverter [J]. *IEEE Transactions on Power Electronics*, 2017, 32(10): 7419-7434.
- [6] W. Jiang et al. A Novel Virtual Space Vector Modulation With Reduced Common-Mode Voltage and Eliminated Neutral Point Voltage Oscillation for Neutral Point Clamped Three-Level Inverter [J]. *IEEE Transactions on Industrial Electronics*, 2020, 67(2): 884-894.
- [7] Hu Cungang, Wang Qunjing, Li Guoli, et al. Midpoint voltage Balance control method of three-level NPC Inverter based on Virtual space vector [J]. *Transactions of China Electrotechnical Society*, 2009, 24(05): 100-107.
- [8] P. Liu, S. Duan, C. Yao and C. Chen. A Double Modulation Wave CBPWM Strategy Providing Neutral-Point Voltage Oscillation Elimination and CMV Reduction for Three-Level NPC Inverters [J]. *IEEE Transactions on Industrial Electronics*, 2018, 65(1): 16-26.
- [9] Gao Zhan, GE Qiongquan, Li Yaohua et al. A carrier-based zero-vector first SVPWM method for three-level midpoint clamp converter [J]. *Transactions of China Electrotechnical Society*, 2019, 35(10): 2194-2205.
- [10] Zhao Hui, Li Rui, Wang Hongjun et al. Research on SVPWM Method of three-level inverter in 60° coordinate system [J]. *Proceedings of the CSEE*, 2008(24): 39-45.
- [11] Zhao Xingchen. Multilevel Driving Technology of permanent magnet synchronous Motor [D]. Jiangsu: Nanjing University of Aeronautics and Astronautics, 2018.
- [12] F. B. Grigoletto and H. Pinheiro. A space vector PWM modulation scheme for back-to-back three-level diode-clamped converters [C]. 2009 Brazilian Power Electronics Conference, Bonito-Mato Grosso do Sul, Brazil, 2009, 1058-1065.
- [13] S. Busquets-Monge, J. Bordonau, D. Boroyevich and S. Somavilla. The nearest three virtual space vector PWM - a modulation for the comprehensive neutral-point balancing in the three-level NPC inverter [J]. *IEEE Power Electronics Letters*, 2004, 2(1): 11-15.
- [14] X. Xing, X. Li, F. Gao, C. Qin and C. Zhang. Improved Space Vector Modulation Technique for Neutral-Point Voltage Oscillation and Common-Mode Voltage Reduction in Three-Level Inverter [J]. *IEEE Transactions on Power Electronics*, 2019, 34(9): 8697-8714.
- [15] Jia Wanshui, Zhang Cheng, Xiong Zichen. Improved Virtual space Vector modulation for NPC three-level Inverter [J]. *Marine Electric Technology*, 2022, 42(04): 18-23.
- [16] Wang Lu, Fan Bo, QIU Yulin. Three-level midpoint potential balance Control based on voltage feedback VSVPWM [J]. *Computer Simulation*, 2022, 39(11): 118-124.
- [17] C. -Q. Xiang, C. Shu, D. Han, B. -K. Mao, X. Wu and T. -J. Yu. Improved Virtual Space Vector Modulation for Three-Level Neutral-Point-Clamped Converter With Feedback of Neutral-Point Voltage [J]. *IEEE Transactions on Power Electronics*, 2018, 33(6): 5452-5464.
- [18] GUI Shi-Weng, Wu Fang, Wan Shan-Ming, et al. Midpoint potential Balance control Strategy of three-level NPC Converter with variable virtual space vector [J]. *Proceedings of the CSEE*, 2015, 35(19): 5013-5021.

About the author: Pang Songhan (2000-), male, Han nationality, born in Liaocheng, Shandong Province, master candidate, research direction is high-speed permanent magnet synchronous motor drive control ;

Liu Jian (1982-), male, Han nationality, born in Chifeng, Inner Mongolia, PhD, associate professor, research direction is permanent magnet motor drive control and converter modulation theory ;

Wu Kuikui (1983-), male, Han nationality, born in Jiaxing, Zhejiang Province, engineer, research direction is high-speed permanent magnet synchronous motor body design and drive ;

Zhang Hongqi (1968-), male, Han nationality, born in Zibo, Shandong Province, engineer, research direction is digital analysis of special motors ;

Note: The corresponding author is Jian Liu.